

# Frequency spectra of magnetostrictive and Lorentz forces generated in ferromagnetic materials by a CW excited EMAT

C Rouge<sup>1,2</sup>, A Lhémy<sup>1</sup> and C Aristégui<sup>2</sup>

<sup>1</sup>CEA, LIST, F-91191 Gif-sur-Yvette cedex, France

<sup>2</sup>Université de Bordeaux, UMR CNRS 5295, I2M/Acoustique Physique, 33405 Talence cedex, France

E-mail: alain.lhemery@cea.fr

**Abstract.** Magnetostriction arises in ferromagnetic materials subjected to magnetization, *e.g.*, when an EMAT (Electro-Magnetic Acoustic Transducer) is used to generate ultrasonic waves. In such a case, the magnetostriction force must be taken into account as a transduction process that adds up to the Lorentz force. When the static magnetic field is high compared to the dynamic field, both forces are driven by the excitation frequency. For lower static relative values of the magnetic fields, the Lorentz force comprises both the excitation frequency and its first harmonic. In this work, a model is derived to predict the frequency content of the magnetostrictive force that comprises several harmonics. The discrete frequency spectrum strongly depends on both the static field and the relative amplitude of the dynamic field. The only material input data needed to predict it is the curve of macroscopic magnetostrictive strain that can be measured in the direction of an imposed magnetic field. Then, the various frequency-dependent distributions of Lorentz and magnetostriction body forces can be transformed into equivalent surface stresses. Examples of computation are given for different static and dynamic magnetic fields to study their influence on the frequency content of waves generated in ferromagnetic materials.

## 1. Introduction

Electro-magnetic acoustic transducers (EMAT) are commonly used in the context of ultrasonic nondestructive testing. They are often used to generate guided waves and more specifically shear horizontal waves in plates or torsional waves in cylinders. In some cases, EMAT efficiency is increased when they are used with magnetostrictive patches or in ferromagnetic materials [1]. The two main processes at the origin of wave generation by an EMAT are the Lorentz and the magnetostriction forces [2, 3]. The first exists in all conductive media while the second is restrictive to ferromagnetic materials. The two forces can be the source of ultrasounds at frequencies different from the excitation frequency. For the Lorentz force, the excitation of waves at a frequency twice the excitation frequency is easily understood, as recalled hereafter. This is more complicated dealing with the magnetostriction force; its frequency spectrum cannot be explicitly given.

The first aim of present work is to model the frequency spectrum of the magnetostriction force. In addition, to compute the amplitude of waves generated by an EMAT in a ferromagnetic material, the magnetostriction and the Lorentz forces are transformed into surface stresses that can be readily used as source terms in existing semi-analytical models of wave radiation of bulk [4] or guided waves [5]. The transformation explained in two previous papers [6, 7] is valid since the two body forces are constrained in the vicinity of the plate surface. The order of magnitude of the equivalent surface stress



of the magnetostriction force is compared to results from the literature. A very good estimation of this quantity is obtained as compared to Ribichini *et al.* [8] finite element results. Then, the contributions of the fundamental and the first four harmonics of the magnetostriction force to SH0 guided mode in a ferromagnetic plate are given as an example of application. The fact that harmonic amplitudes cannot be always neglected is clearly illustrated.

## 2. Frequency spectra of the electromagnetic forces

### 2.1. Magnetic field created by an EMAT

The Lorentz force  $\mathbf{F}_L$  results from the interaction of eddy currents  $\mathbf{J}$  created in the material by the EMAT coil and the magnetic induction field  $\mathbf{B}$  generated by both the permanent magnet and the coil. It is expressed as follows

$$\mathbf{F}_L = \mathbf{J} \times \mathbf{B}. \quad (1)$$

If the magnetic induction field is decomposed into a static field  $\mathbf{B}_S$  and a dynamic one  $\mathbf{B}_D e^{j\omega_0 t}$ , the Lorentz force can be re-written as

$$\mathbf{F}_L = \mathbf{J}_D \times \mathbf{B}_S e^{j\omega_0 t} + \mathbf{J}_D \times \mathbf{B}_D e^{2j\omega_0 t}, \quad (2)$$

where eddy currents are pure dynamic quantities with  $\mathbf{J} = \mathbf{J}_D e^{j\omega_0 t}$  and where a harmonic excitation of angular frequency  $\omega_0$  is considered. This expression highlights the two interactions at its origin. The first is that of eddy currents generated in the material by the coil with the static magnetic field due to the permanent magnet; it is given by the first term of the right hand side of equation (2) and involves a  $e^{j\omega_0 t}$  factor. Eddy currents also interact with the dynamic magnetic field; this is expressed by the second term proportional to  $e^{2j\omega_0 t}$ . If the dynamic magnetic field is not negligible compared to the static one, the double frequency effect appears.

### 2.2. Calculation of the magnetostrictive strain coefficients

As formulated by Thompson [1] and Ogi [2], the calculation of the magnetostriction force reduces to the evaluation of the magnetostrictive strain coefficients. Two 2D cases have to be considered in order to form the complete magnetostrictive strain tensor in 3D.

**2.2.1. Dynamic magnetic field collinear with the static magnetic field.** The first case to consider is when the static magnetic field  $\mathbf{H}_S$  and the dynamic one  $\mathbf{H}_D$  are collinear, as shown in Figure 1 (left). The static field induces a static magnetostrictive strain.

This fixed value is shown in Figure 1 (right) on the magnetostriction curve  $\varepsilon(H)$  [2] that represents the magnetostrictive strain due to a magnetic field. This curve shown is typical of steels. A superimposed dynamic field produces time-dependent oscillations of the magnetostrictive strain around this fixed value. Thus, the total excitation field  $\mathbf{H}_T$  (static plus dynamic fields) induces a time-dependent magnetostrictive strain  $\varepsilon_T$ .

To express the magnetostrictive strain vector in a plane containing the two magnetic fields, two assumptions are made. The first one is that the magnetostriction curve, Figure 1 (right), is the same at any point of the material studied for any applied magnetic field direction. The second is that the magnetostriction effect keeps the material volume constant. Under these two assumptions, the magnetostrictive strain vector is written as

$$\boldsymbol{\epsilon}_{\text{MS}} = \begin{pmatrix} \epsilon_T \\ -\frac{1}{2}\epsilon_T \\ -\frac{1}{2}\epsilon_T \\ 0 \\ 0 \\ 0 \end{pmatrix}. \quad (3)$$

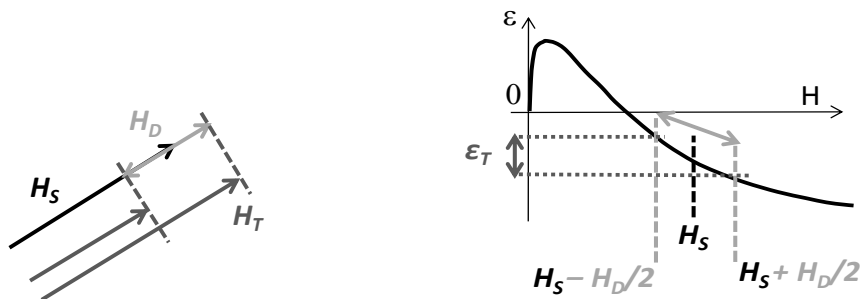


**Figure 1:** Case 1: the static and the dynamic magnetic fields are collinear (left); they induce different magnetostrictive strains represented on the magnetostriction curve (steels) (right).

These two assumptions are not restrictive in the context of NDT by EMAT in regards of typical materials tested and magnetic field amplitudes used. As far as the first is concerned, it is a consequence of magnetic isotropy that is observed in disordered materials. The second assumption can be made unless very high magnetization fields are generated; for example, it applies very well for a field of 0.5 T (see Bozorth [9]) which is already quite large for an EMAT used in NDT.

**2.2.2. Dynamic magnetic field perpendicular to the static magnetic field.** The case where the static and the dynamic excitation fields are not collinear is now considered. For example, the static field is aligned along the  $\mathbf{x}$ -axis and the dynamic one is perpendicular to it, as shown on Figure 2. The total field is thus applied in the resulting direction, denoted by  $\mathbf{x}'$ , which is time-dependent, making an angle  $\theta$  with the static field direction.

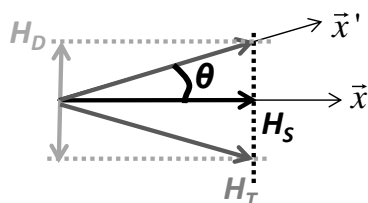


**Figure 2:** Case 2: the static and the dynamic magnetic fields are perpendicular.

Under the same assumptions as made in § 2.2.1, the magnetostrictive strain vector in the  $\mathbf{x}'$  direction is expressed similarly as in equation (3), but with another total strain denoted by  $\epsilon_T^{xy}$ . A rotation of angle  $\theta$  must be further applied to express it in the absolute coordinates. One gets

$$\boldsymbol{\varepsilon}_{\text{MS}} = \begin{pmatrix} \varepsilon_T^{xy} \cos^2(\theta) - \frac{1}{2} \varepsilon_T^{xy} \sin^2(\theta) \\ -\frac{1}{2} \varepsilon_T^{xy} \cos^2(\theta) + \varepsilon_T^{xy} \sin^2(\theta) \\ -\frac{1}{2} \varepsilon_T^{xy} \\ 0 \\ 0 \\ \frac{3}{2} \varepsilon_T^{xy} \sin(2\theta) \end{pmatrix}. \quad (4)$$

2.2.3. *Magnetostrictive strain tensor.* Finally, if the static field direction is along the  $\mathbf{x}$  axis, the magnetostriction strain tensor is readily written as

$$\boldsymbol{\varepsilon}_{\text{MS}} = \begin{pmatrix} \varepsilon_T & \varepsilon_T^{xy} \cos^2(\theta_{xy}) - \frac{1}{2} \varepsilon_T^{xy} \sin^2(\theta_{xy}) & \varepsilon_T^{xz} \cos^2(\theta_{xz}) - \frac{1}{2} \varepsilon_T^{xz} \sin^2(\theta_{xz}) \\ -\frac{1}{2} \varepsilon_T & -\frac{1}{2} \varepsilon_T^{xy} \cos^2(\theta_{xy}) + \varepsilon_T^{xy} \sin^2(\theta_{xy}) & -\frac{1}{2} \varepsilon_T^{xz} \\ -\frac{1}{2} \varepsilon_T & -\frac{1}{2} \varepsilon_T^{xy} & -\frac{1}{2} \varepsilon_T^{xz} \cos^2(\theta_{xz}) + \varepsilon_T^{xz} \sin^2(\theta_{xz}) \\ 0 & 0 & 0 \\ 0 & 0 & \frac{3}{2} \varepsilon_T^{xz} \sin(2\theta_{xz}) \\ 0 & \frac{3}{2} \varepsilon_T^{xy} \sin(2\theta_{xy}) & 0 \end{pmatrix}, \quad (5)$$

where the first column represents the magnetostrictive strain along the  $\mathbf{x}$  axis with a total deformation in this direction denoted by  $\varepsilon_T$ ; the second represents the magnetostrictive strain in the  $(\mathbf{x}, \mathbf{y})$  plane with a total deformation  $\varepsilon_T^{xy}$  in the direction of the total magnetic field and an angle  $\theta_{xy}$  between the  $\mathbf{x}$ -axis and the direction of the total magnetic field. Accordingly, the third represents the magnetostrictive strain in the  $(\mathbf{x}, \mathbf{z})$  plane with a total deformation  $\varepsilon_T^{xz}$  and an angle  $\theta_{xz}$ . The various quantities appearing in equation (5) are time-dependent.

### 2.3. Magnetostriction force frequency spectrum

From the previous strain expression, the magnetostriction force can be calculated. Five steps are necessary. The first consists in calculating the piezomagnetic strain tensor  $\mathbf{d}$ , given by

$$d_{ij} = \frac{\partial \varepsilon_{MS_i}}{\partial H_j}. \quad (6)$$

Next, the piezomagnetic stress tensor  $\mathbf{e}$  is calculated with the help of the elastic stiffness tensor  $\mathbf{C}$ :

$$\mathbf{e} = \mathbf{C} \mathbf{d}. \quad (7)$$

Then, the magnetostrictive stress tensor  $\boldsymbol{\sigma}_{\text{MS}}$  is expressed by

$$\boldsymbol{\sigma}_{\text{MS}} = -\mathbf{e} \mathbf{H}. \quad (8)$$

The stress free boundary conditions at the part surface are accounted for in the calculation of the magnetostrictive stress tensor by writing

$$\boldsymbol{\sigma}_{\text{MS}} \cdot \mathbf{n} = 0. \quad (9)$$

Finally, the magnetostriction force  $\mathbf{F}_{\text{MS}}$  is expressed by

$$\mathbf{F}_{\text{MS}} = \nabla \cdot \boldsymbol{\sigma}_{\text{MS}}. \quad (10)$$

The frequency content of the magnetostriction force does not explicitly appear in this formulation. Its evaluation is made by means of the following algorithm, schematized by Figure 3.

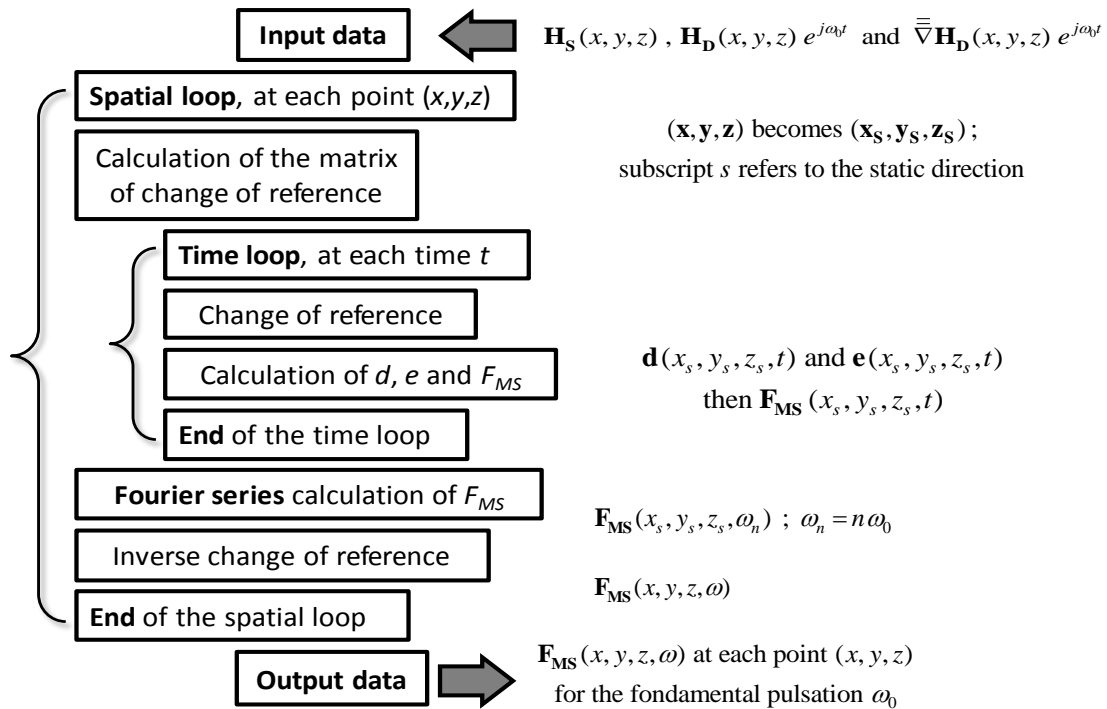


**Figure 3:** Calculation of the magnetostriction force frequency spectrum for a harmonic excitation  $\omega_0$ .

For a given CW excitation of angular frequency  $\omega_0$ , the magnetic fields  $\mathbf{H}_s$  and  $\mathbf{H}_d$  are computed. They constitute the input of the calculation. At each point  $(x, y, z)$  in the global reference system  $(\mathbf{x}, \mathbf{y}, \mathbf{z})$ , a local reference system  $(\mathbf{x}_s, \mathbf{y}_s, \mathbf{z}_s)$  is used: the first axis  $\mathbf{x}_s$  coincides with the static field direction at the point considered. Previous expressions of  $\boldsymbol{\varepsilon}_{\text{MS}}$  can thus be readily used. Next, the magnetostriction force is calculated in the time domain. This is done in a time loop over one period of the excitation frequency. At the end of this time-loop, the frequency spectrum of the magnetostriction force is calculated thanks to a Fourier series, and is finally expressed in the global reference system. At the end of the algorithm, the frequency spectrum is computed at all the calculation points for a given excitation frequency.

#### 2.4. Examples of spectra

Let us now consider examples of frequency spectra of magnetostriction force. The magnetostriction curve used is that previously shown in Figure 1 (right), [2].

Three static field intensities are considered corresponding respectively to a weak, a moderate and a high bias field induction of  $0.5$ ,  $2$  and  $6.5 \cdot 10^4 \text{ A.m}^{-1}$ , respectively (see Figure 4). Three dynamic field intensities are also considered:  $0.1$ ,  $0.5$  and  $1 \cdot 10^4 \text{ A.m}^{-1}$ . The frequency spectra of a point situated at the plate surface below the middle of a wire are represented in Figure 5. They are normalized with

respect to their highest component. Results show a general behaviour already described in the literature [10]: harmonics are negligible for high static fields; their amplitude relatively to that of the fundamental increases with decreasing static fields. The non linear behaviour of the force is at its highest as shown at the right top of Figure 5, for a low static field and a high dynamic field.

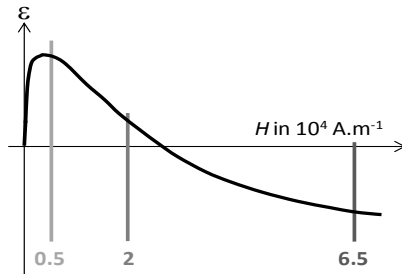


**Figure 4:** Steel magnetostriction curve, used for the examples of magnetostriction frequency spectra; the three static field amplitudes used are shown.

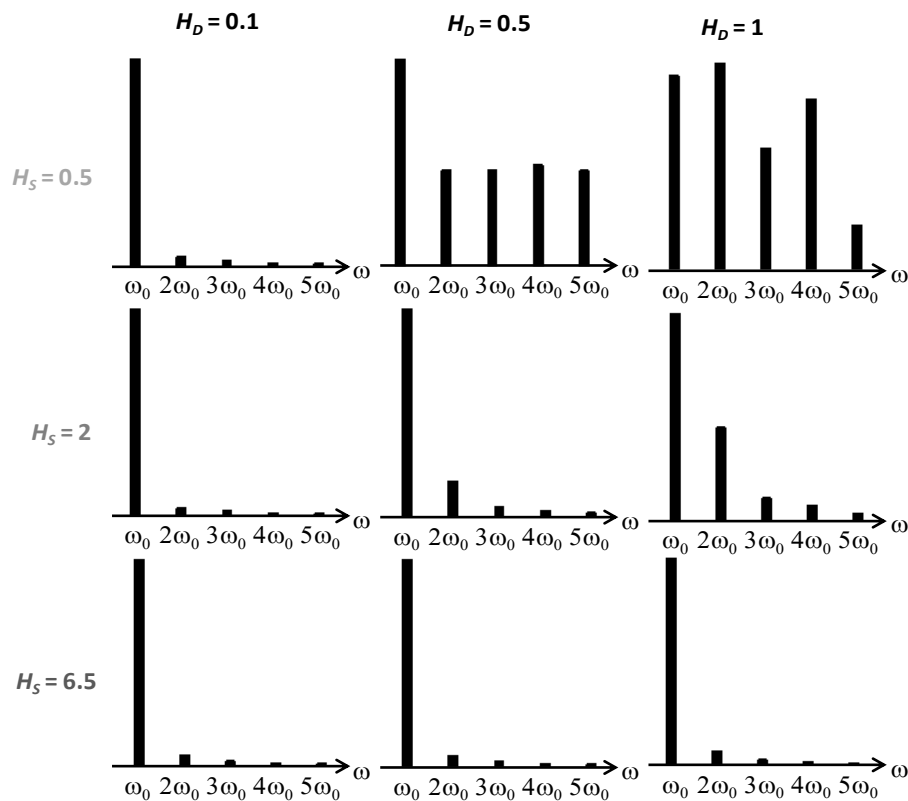


**Figure 5:** Normalized spectra of the magnetostriction force for different amplitudes of static and dynamic magnetic fields. Amplitudes in  $10^4 \text{ A.m}^{-1}$ .

The described algorithm allows one to compute frequency spectra associated to the magnetostriction force, extended to deal with arbitrary value of the bias field. This is a key point of our modelling approach since a high bias field assumption is generally made in existing theoretical modelling of magnetostriction. Moreover, the modelling relies on the knowledge of only one material input data, the macroscopic magnetostriction curve, which is easily measured experimentally.

### 3. Generation of guided waves by an EMAT in a ferromagnetic plate

#### 3.1. Transformation of body forces into equivalent surface stresses

Thanks to the developments made in the previous section, the Lorentz and magnetostriction forces are calculated as frequency spectra in the volume of the part. These body forces are now considered as source terms in the equation of motion describing the elastic wave generation and propagation in the

part. This is classically achieved by means of a convolution integral over the part volume of the source with the elastodynamic Green's tensor for the problem in hands.

By integrating the Lorentz force over the depth, that is, in the direction normal to the surface where the EMAT is applied, the volume integral can be transformed into a simpler surface integral [3,11]; this leads to the definition of a distribution of sources of surface stresses which approximately radiates the same wavefield as that radiated by the body force distribution. Proceeding to such a transform is computationally more efficient; moreover, the equivalent surface stress can be readily used in various existing models of wave radiation.

Unfortunately, such a simple integration scheme has been shown (Thompson [1,12]) to lead to a non-physical result when applied to the magnetostriction force, since the depth integral of this force vanishes. A more complicated integration scheme has been developed by Thompson [12] to overcome this difficulty. In two previous papers published in this series [6,7], Thompson's method has been reused. Final results in Thompson's paper were partly mistyped; we worked out the whole derivation of this transformation in details; this is rather technical and long and out of the scope of the present paper. The transformation may be found in [13] to which interested readers are referred.

### 3.2. Comparison with results from the literature

As far as Lorentz and magnetostriction forces are concerned, persistent discussions on their relative amplitude were found in the literature. In a recent joint paper by Ribichini, Nagy and Ogi [8], the magnetostriction force computed by Ribichini using a finite element method is compared to that computed by Hirao and Ogi [2] by means of an analytical expression of the force. In [2], boundary conditions of free surface were not taken into account. In the joint paper [8], the magnetostriction force for generating SH waves was considered and Ogi admitted that his results were wrong.

For validation purposes, the same case has been treated using our own modelling approach, consisting in computing the equivalent surface stress of the magnetostriction force; our results are compared to the various results given in [8]. As shown by Table 1, two or three orders of difference are found between Hirao and Ogi's model [2] and Ribichini's results. Our own results are of the same order as Ribichini's finite element results.

**Table 1:** Comparison of the order of magnitude of equivalent magnetostriction surface stress given by Hirao and Ogi [2], Ribichini *et al.* [8] and computed by the present method.

	Calculation method of the force	Magnitude of equivalent surface stress
Hirao and Ogi [2]	$\sigma_{MS} = \mathbf{e} \mathbf{H}$	$10^1$ to $10^2$
Ribichini <i>et al.</i> [8]	finite element	$10^{-1}$
present method	$\begin{cases} \sigma_{MS} = \mathbf{e} \mathbf{H} \\ \sigma_{MS} \cdot \mathbf{n} = 0 \end{cases}$	$10^{-1}$

## 4. Results and discussion

Combining the calculation of both the Lorentz and the magnetostriction forces, their transformation into equivalent surface stresses and two models for predicting guided waves radiated by surface stresses (SH [6] and Lamb waves [7]), the modal amplitudes of guided waves generated by an EMAT into a ferromagnetic plate can be computed.

Here, an example of SH modal amplitude variation with the excitation frequency is given. The configuration used is shown on Figure 6 (left) and consists in a meander-coil associated to a tangential static magnetization. The 3-mm-thick plate is made of iron, characterized by the magnetostriction curve given by Hirao and Ogi [2] shown on Figure 6 (right).

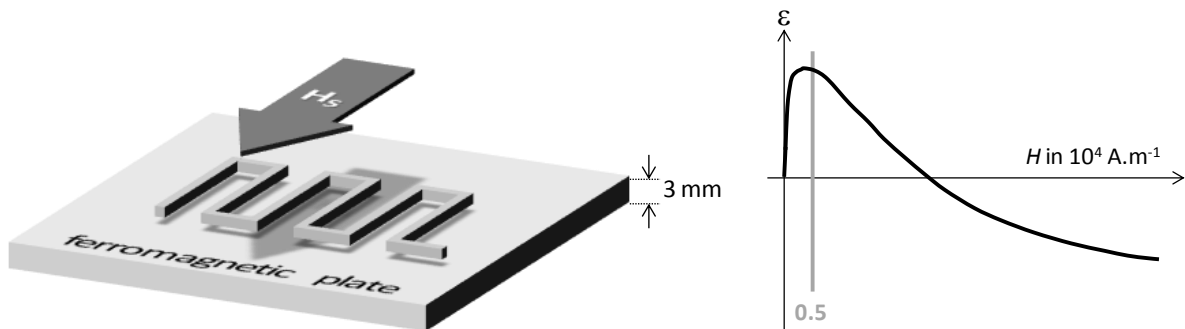


**Figure 6:** Left: EMAT configuration for generating SH waves. Right: magnetostriction curve used.

The modal amplitude of the first SH mode, SH0, is studied as function of the frequency for two current intensities (a low one of 40A and a high one of 400A). The left graph of figure 7 is computed for the low intensity of 40A, the right for the high intensity of 400A. Only the magnetostriction force is considered. Two different kinds of results are shown and superimposed on the same figure 7.

The first series (dark blue circles) represents the SH0 modal amplitude of the fundamental component of the magnetostriction force, over a frequency range from 0.1 to 1.0 MHz (note that the whole range is below the first cut-off frequency of SH guided waves in the plate considered).

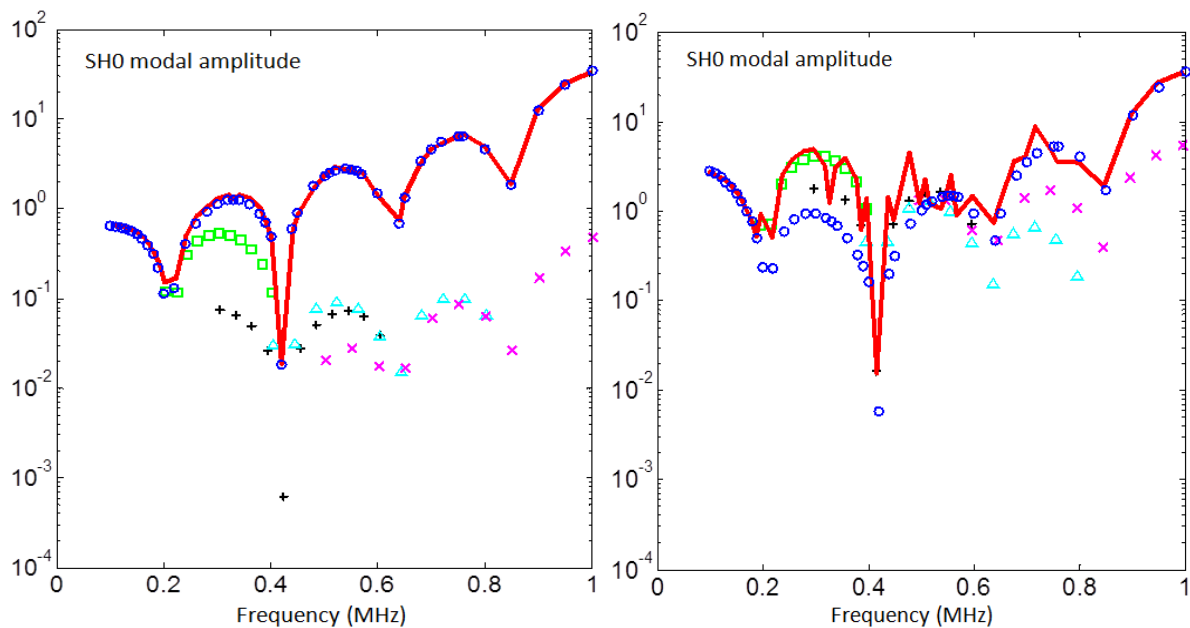


**Figure 7:** Left: 40A intensity; right: 400A.  $\circ$ : SH0 amplitude due to the fundamental component of the magnetostriction force in the range [0.1 - 1] MHz.  $\square$  (resp.  $+$ ,  $\triangle$ ,  $\times$ ) contribution of 1<sup>st</sup> (resp. 2<sup>nd</sup>, 3<sup>rd</sup> and 4<sup>th</sup>) harmonic to the SH0 amplitude for a fundamental excitation in the range [0.1 - 0.2] MHz. Red curve: total amplitude of the SH0 mode for a fundamental excitation in the range [0.1 - 0.2] MHz.

The second series of results represents the SH0 modal amplitude of the first four harmonic contributions of the magnetostriction force, considering a fundamental excitation frequency varying in the 0.1-0.2 MHz frequency range. Therefore, the frequency range covered by these harmonics varies from 0.2 to 1.0 MHz. The various contributions are displayed separately (see figure caption). For the same excitation ([0.1-0.2] MHz), the fundamental and harmonic contributions are summed and the resulting amplitude is displayed as a red line.

In both graphs, a log-scale is used for the wave amplitude. Comparing the first series (blue circles) to the last (red line) allows us to quantify the effect of harmonic contributions. For a low intensity (left), both series almost superimpose: harmonics make a negligible contribution in this case. This is



easily seen by looking closely at the individual contributions of the various harmonics; only the first harmonic in the range 0.2-0.4 MHz (green squares) slightly modifies the overall amplitude. A totally different behaviour is seen for high intensity (right graph). All over the frequency range of harmonics [0.2-1.0] MHz, contributions of the first four harmonics clearly cannot be neglected.

These results, obtained in a rather simple configuration, exemplify the ability of our approach to predict contributions of magnetostrictive forces in a wide variety of cases in terms of relative amplitude of static and dynamic magnetic fields. Our approach makes it possible to choose arbitrary values of bias field and of current intensity while most works make the restrictive assumptions of high bias field and low current intensity, the main reason for such restrictions being the difficulty to model the generation of harmonics by magnetostrictive effect.

## Conclusions

A model has been proposed to compute the elastodynamic source terms associated to the magnetostriction force generated by an EMAT in a ferromagnetic part. Compared to existing semi-analytical models of magnetostriction, the present model can deal with arbitrary values of bias field and of current intensity thus with arbitrary EMAT design. This capability results from the specific development of a method to predict the complex-valued amplitude of contributions associated to harmonic frequencies of the fundamental excitation frequency. These contributions are negligible if high bias field and low current intensity are concerned, as shown by our results and as it is well established. Contributions from harmonics can however surpass that of the fundamental, as exemplified by our results dealing with a high current intensity. The present model can therefore help designing new EMAT for new applications.

Thanks to a mathematical method detailed in [13], the Lorentz and magnetostrictive body force distributions can be transformed into surface stress distributions. Finally, combining the calculation of force spectra with the transformation method of force into stress, the contributions of the fundamental excitation frequency and of its harmonics for both the Lorentz and the magnetostriction forces to any propagative mode (guided, bulk and surface waves) can be calculated.

Future work will include the calculation of non linear magnetic fields induced in the material. Accounting for non linear permeability shall increase the accuracy of the magnetic field calculation, thus, of the input data of the present model.

## References

- [1] Thompson R B 1978 *I.E.E.E. Trans. Son. Ultrason.* **SU-25** 7–15
- [2] Hirao M and Ogi H 2003 *EMATS for Science and Industry: Noncontacting Ultrasonic Measurements* (Boston: Kluwer Academic Publishers)
- [3] Thompson R B 1990 Physical principles of measurements with EMAT transducers *Physical Acoustics* vol 19 (New-York: Academic Press) chapter 4 pp 157–200
- [4] Lhémy A 1994 *J. Acoust. Soc. Am.* **96** 3776–86
- [5] Ditre J J and Rose J F 1992 *J. Appl. Phys.* **72** 2589–97
- [6] Rouge C, Lhémy A and Ségur D 2012 *J. Phys.: Conf. Ser.* **353** 012014
- [7] Rouge C, Lhémy A and Aristégui C 2013 *J. Phys.: Conf. Ser.* these proceedings.
- [8] Ribichini R, Nagy P B and Ogi H 2012 *NDT&E Int.* **51** 8–15
- [9] Bozorth R M 1964 *Ferromagnetism* (Hoboken: Wiley-Interscience)
- [10] Laguerre L, Aime J-C and Brissaud M 2002 *Ultrasonics* **39** 503–14
- [11] Kawashima K 1984 *I.E.E.E. Trans. Son. Ultrason.* **SU-31** 83–94
- [12] Thompson R B 1980 *J. Nond. Eval.* **1** 79–85
- [13] Rouge C, Lhémy A and Ségur D 2013 *J. Acoust. Soc. Am.* **134** 2639-46